Journal of Sound and Vibration (2001) **241**(2), 328–336
doi:10.1006/jsvi.2000.3246, available online at http://www.idealibrary.com on IDEAL®

A SPLINE JOINT FORMULATION FOR DRIVE TRAIN TORSIONAL DYNAMIC MODELS

A. KAHRAMAN

Center for Gear Research, The University of Toledo, Toledo, OH 43606-3390, *U.S.A.*
E-mail: akahrama@eng.utoledo.edu

(*Received* 11 *July* 2000)

1. INTRODUCTION

Splines are used commonly in drive train applications to connect components carrying torque such as shafts, gears, clutches, couplings and other structures including planetary carriers. As a simple example of a spline joint in a drive train application, consider a shaft-gear pair shown in Figure 1. Here, both the shaft and the gear (or any other component splined to the shaft) are assumed to deflect only at the spline teeth. A total number of n external teeth machined on the shaft mate with n internal groves at the bore of the gear forming a positive engagement between two bodies ensuring proper transfer of the torque.

For an idealized case when there is no clearance (backlash) between the two bodies as in the *side-bearing-fit*-type splines [1] and the teeth are machined with no circumferential position (spacing or indexing) errors, all n teeth will be in contact sharing equal amounts of load. In this ideal case, the torsional stiffness of the spline joint is constant, and it is significantly larger than other stiffness values in the system such as those of the gear mesh and shaft torsion. In such cases, it is customary to neglect the flexibility of the spline joint in torsional dynamic models assuming that the shaft is rigidly connected to the gear. Meanwhile, a great majority of the real-life automotive, aerospace and industrial applications differ from the above-idealized case for two reasons. First of all, most spline joints have backlash that is designed primarily for assembly purposes, as it is the case in *major diameter-fit* and *minor diameter-fit*-type splines [1]. This introduces a clearance-type non-linearity similar to the other common mechanical components such as gear pairs, linkages, rolling element bearings, clutches and couplings (see, e.g., references [2–8]) even if all spline teeth are spaced equally and are of equal thickness. Secondly, the circumferential tooth position errors originated from the machining process and heat treatment distortions prevent each teeth from coming into contact at the same time resulting in a torsional stiffness coefficient that is dependent on the amplitude of the relative displacement.

In modelling drive trains, spline joints have traditional been assumed to be rigid. To this author's best knowledge, the literature lacks any generalized and practical formulation of a spline joint that includes the common features such as clearance (backlash) and circumferential tooth flank position errors. Accordingly, the objective of the communication is to propose a piecewise linear dynamic model of a spline joint subjected to both backlash and tooth position errors. The equation of motion and the piecewise linear displacement function will be obtained in dimensionless form. For cases with a large

0022-460X/01/120328 + 09 $35.00/0

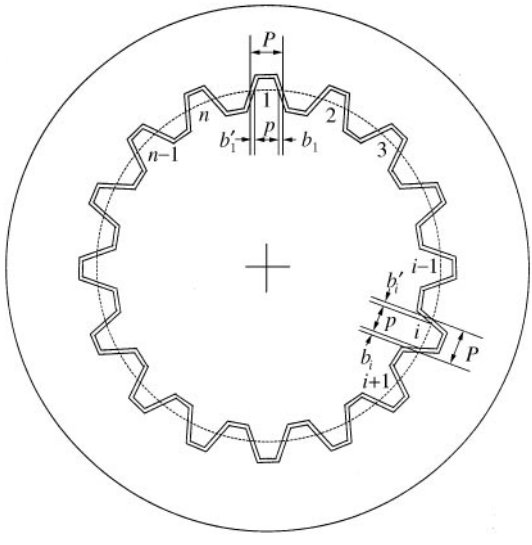

Figure 1. A shaft-gear pair with a spline joint.

number of spline teeth, a generalized approximation that reduces the piecewise linear displacement function into a piecewise non-linear one will be proposed. Accuracy of this approximation will be demonstrated using a case of linearly varying tooth spacing errors.

2. FORMULATION

For a general case when the spline contains both backlash and tooth spacing errors, each tooth of the external spline i has a different amount of clearance at the front (loaded) and back flanks, b_i and b_i', respectively, as shown in Figure 1. As a result of this, when the joint is loaded, first the tooth with smallest clearance should come to contact followed by the others in an order based on the magnitude of their clearance values. Then, only a portion of n teeth at the joint will be in contact if the mean torque transmitted results in spline tooth deflections less than the largest clearance in the system. This results in a piecewise linear displacement function in the regime where the number of teeth in contact r is less than the total number of spline teeth, n.

The equation of motion of the gear splined compliantly to a shaft as shown in Figure 1 is given as

$$I\frac{\mathrm{d}^2\theta}{\mathrm{d}t^2} + c_t\frac{\mathrm{d}\theta}{\mathrm{d}t} + k_t g[\theta(t)] = T(t), \tag{1}$$

where I is the polar mass moment of inertia of the gear, c_t is the overall torsional viscous damping coefficient of the spline joint, k_t is the torsional stiffness due to a single spline tooth contact, $\theta(t)$ is the angular displacement of the gear, and $T(t)$ is the torque acting on the gear including its mean and alternating components. The non-linear displacement function $g[\theta(t)]$ that will be defined later is employed to represent the non-linearities caused by the spacing errors and overall spline backlash. The equation of motion can be put in the following standard format by introducing $\omega_n^2 = k_t/I$ and $\zeta = c_t/(2I\omega_n)$:

$$\frac{\mathrm{d}^2\theta}{\mathrm{d}t^2} + 2\zeta\omega_n\frac{\mathrm{d}\theta}{\mathrm{d}t} + \omega_n^2 g[\theta(t)] = \frac{T(t)}{I}. \tag{2}$$

In order to describe the problem in hand more clearly, one can consider the equivalent translational model shown in Figure 2, in which the rotational components are replaced by the equivalent translational components. Now, an n number of cantilever teeth mounted on a block representing the gear are lined up in a row against grooves on another block representing the shaft that is held stationary. With the translational displacement $y(t) = r_p\theta(t)$ as the new coordinate, where r_p is the pitch circle radius of the spline, equation (2) is rewritten as

$$\frac{\mathrm{d}^2y(t)}{\mathrm{d}t^2} + 2\zeta\omega_n\frac{\mathrm{d}y}{\mathrm{d}t} + \omega_n^2 g[y(t)] = f(t), \tag{3}$$

where $f(t) = r_pT(t)/I$. The displacement function $g[y(t)]$ is formed by n individual piecewise-linear displacement functions $g_i[y(t)]$ shown in Figure 2, each representing one of the teeth in the interface. Given constant values of tooth thickness of the external spline p and the magnitude of the internal spline gap P, the clearances of tooth i at the right (loaded) and left (unloaded) flanks must satisfy the condition

$$b_i + b_i' = P - p, \quad i = 1, 2, \ldots, n. \tag{4}$$

Since the system is one dimensional, the spline teeth can be sorted based on their clearance such that

$$b_n \geqslant b_{n-1} \geqslant \cdots \geqslant b_3 \geqslant b_2 \geqslant b_1 = a. \tag{5}$$

Then, given equations (4) and (5), the clearances on the left flanks must satisfy the conditions

$$b_1' \geqslant b_2' \geqslant b_3' \geqslant \cdots \geqslant b_{n-1}' \geqslant b_n' = a. \tag{6}$$

It is clear from equations (5) and (6) that the lower block in Figure 2 is in a relative initial position such that there is an equal amount of minimum clearance a at both sides indicating that the total backlash is equal to $2a$. By defining $\beta_i = b_i - a$ and $\beta_i' = b_i' - a$, $i = 1, 2, \ldots, n$, one obtains

$$\beta_n \geqslant \beta_{n-1} \geqslant \cdots \geqslant \beta_3 \geqslant \beta_2 \geqslant \beta_1 = 0, \quad \beta_1' \geqslant \beta_2' \geqslant \beta_3' \geqslant \cdots \geqslant \beta_{n-1}' \geqslant \beta_n' = 0. \tag{7a, b}$$

Accordingly, when $|y(t)| < a$, none of the teeth are in contact resulting in $g[y(t)] = 0$ in equation (3). Similarly, for $(\beta_n + a) \leqslant y(t)$ or $-(\beta_1' + a) \geqslant y(t)$ all teeth are in contact

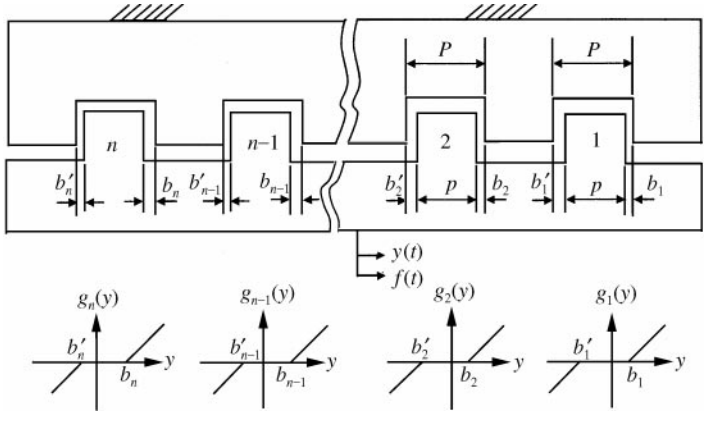

Figure 2. The equivalent translational model of a spline.

resulting is a linear $g[y(t)]$. However when $y(t)$ is such that none of the above conditions are met, then the number of loaded teeth r is less than n and hence $g[y(t)]$ is characterized by a piecewise linear function. With all possible values of $y(t)$, $g[y(t)]$ becomes

$$g[y(t)] = \begin{cases} n[y(t) - a] - \sum_{i=1}^{n} \beta_i, & (\beta_n + a) \leqslant y(t), \\ r[y(t) - a] - \sum_{i=1}^{r} \beta_i, & a \leqslant y(t) < (\beta_r + a), \\ 0, & -a < y(t) < a, \\ -r[|y(t)| - a] + \sum_{i=1}^{r} \beta'_{n+1-i}, & -(\beta'_{n-r} + a) < y(t) \leqslant -a, \\ -n[|y(t) - a] + \sum_{i=1}^{n} \beta'_i, & y(t) \leqslant -(\beta'_1 + a). \end{cases} \tag{8}$$

A dimensionless form of the equation of motion (3) can be obtained by introducing a dimensionless time $\tau = \omega_n t$ and a dimensionless displacement $x(t) = y(t)/a$:

$$\ddot{x}(\tau) + 2\zeta\dot{x}(\tau) + G[x(\tau)] = F(\tau), \tag{9a}$$

$$G[x(t)] = \begin{cases} n[x(\tau) - 1] - \sum_{i=1}^{n} \alpha_i, & (\alpha_n + 1) \leqslant x(\tau), \\ r[x(\tau) - 1] - \sum_{i=1}^{r} \alpha_i, & 1 \leqslant x(t) < (\alpha_r + 1), \\ 0, & -1 < x(\tau) < 1, \\ -r[|x(\tau)| - 1] + \sum_{i=1}^{r} \alpha'_{n+1-i}, & -(\alpha'_{n-r} + 1) < x(\tau) \leqslant -1, \\ -n[|x(\tau)| - 1] + \sum_{i=1}^{n} \alpha'_i, & x(\tau) \leqslant -(\alpha'_1 + 1), \end{cases} \tag{9b}$$

where $\alpha_i = \beta_i/a$ and $\alpha'_i = \beta'_i/a$, $i = 1, \ldots, n$. In Figure 3, the dimensionless form of an equivalent translational spring-mass system is shown, and $G[x(\tau)]$ is illustrated qualitatively to demonstrate each regime forming equation (9b).

3. APPROXIMATE FORM OF THE DISPLACEMENT FUNCTION

Although equation (9) represents a spline joint with backlash and circumferential tooth position errors accurately, its direct use presents difficulties, especially for splines with a large number of teeth n. Each one of the two piecewise linear regions of $G[x(\tau)]$ shown in Figure 3(b) is divided into $n - 1$ linear segments. Accordingly, $G[x(\tau)]$ in equation (9b) is defined by a total of $2n + 1$ such segments including the backlash. For instance, for a spline with $n = 20, 41$ individual piecewise linear segments define $G[x(\tau)]$. In addition, number of teeth in contact r is dependent on the amplitude of $x(\tau)$, which complicates the implementation of equation (9b) even further. Therefore, it is rather impractical to use the exact form of $G[x(\tau)]$ unless n is relatively small, say $n < 5$.

For large n, the piecewise linear regions of $G[x(\tau)]$ shown in Figure 3(b) can be approximated by continuously nonlinear functions [9]. In Figure 4, the contacts on the right tooth flank of the translational model shown in Figure 3(a) are reproduced by defining

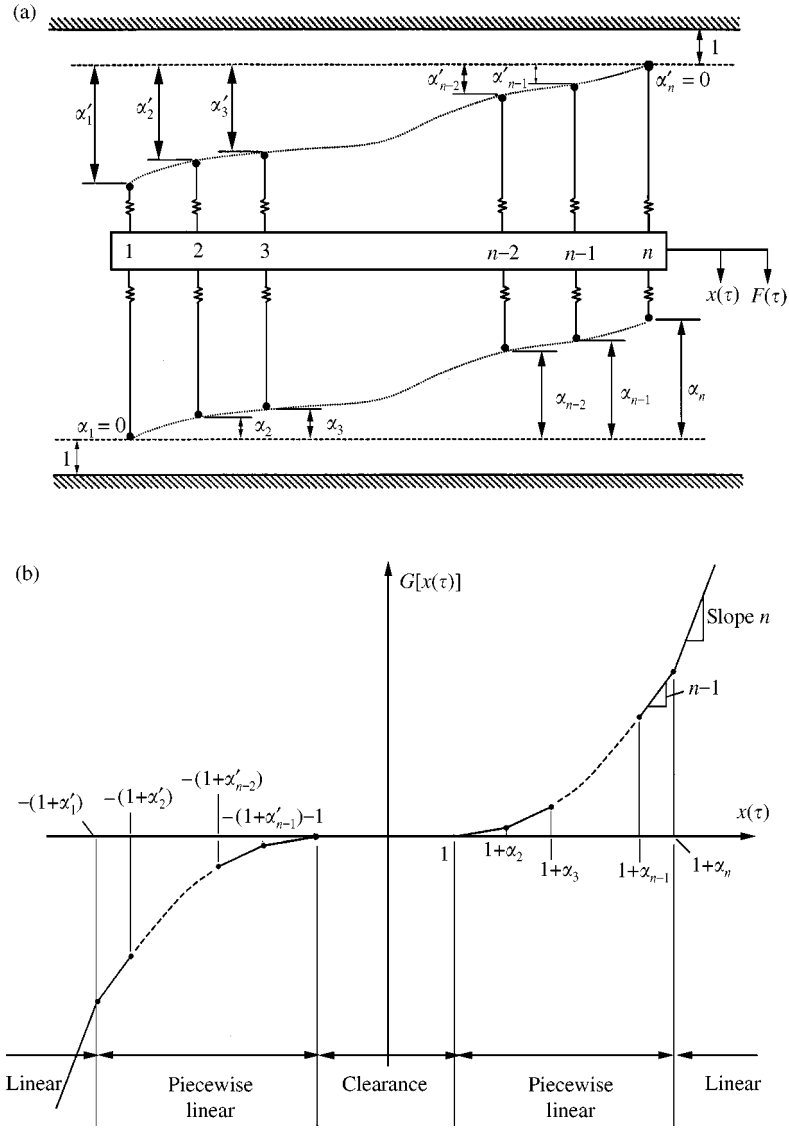

Figure 3. (a) Dimensionless translational representation of a spline with arbitrary tooth spacing errors; (b) graphical illustration of the piecewise linear displacement function $G[x(\tau)]$.

$x' = x - 1$ and another z-axis perpendicular to the x'-axis. Here, the stiffness of each spring is distributed over a length $1/n$ along the z-axis. For any given displacement x', the area of the region between x'-axis and the stepwise profile defined by the ends of the unstretched springs (shaded area) represents the exact value of the displacement function. Approximating the stepwise profile as a continuous function $z = H(x')$, the same area can be described as

$$G[x'(\tau)] = n \int_0^{x'} H(x')\,\mathrm{d}x'. \tag{10}$$

By applying the above equation to any given tooth position error configuration, the piecewise linear regions of Figure 3(b) can be replaced by continuous non-linear functions.

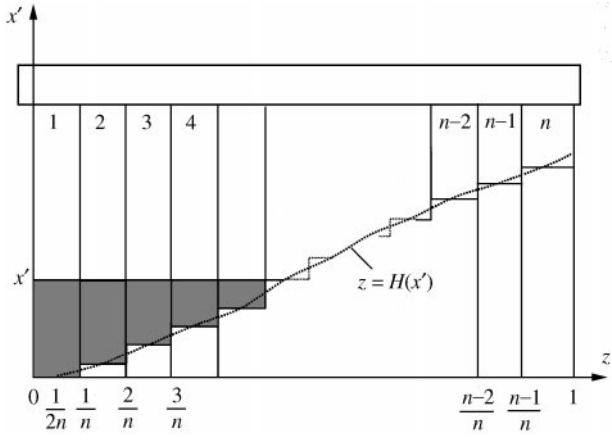

Figure 4. Illustration of the approximation to the piecewise linear $G[x(\tau)]$. Only the right flanks of the teeth are shown for clarity.

Using the current spline inspection techniques available, an approximate of $z = H(x')$ can be determined by inspecting a small portion of the n teeth in the spline joint, making the use of equation (10) even more practical.

In order to demonstrate how to use equation (10), consider a case of uniformly varying tooth position errors illustrated in Figure 5. Such errors result when the spacing angle of the teeth on one the mating spline parts (the gear or the shaft) is machined consistently larger (or smaller) than the nominal dimension. When such a splined part mates with an accurate counterpart, the spacing errors follow a uniform, linearly varying pattern as shown in Figure 5, i.e., $\alpha_i = (i-1)\alpha$. Consequently, the approximate profile $z = H(x')$ is a straight line given as

$$z = H(x') = \frac{1}{n}\left(\frac{x'}{\alpha} + \frac{1}{2}\right), \tag{11}$$

yielding the approximate form of the displacement function in piecewise linear regions for positive values of $x' = x - 1$:

$$G[x(\tau)] = \frac{(x-1)^2}{2\alpha} + \frac{(x-1)}{2}. \tag{12}$$

Using the same formulation for negative values of $x' = x - 1$, the exact form of $G[x(\tau)]$ given in equation (9b) can be approximated by the piecewise non-linear function

$$G[x(\tau)] = \begin{cases} n[x(\tau)-1] - \dfrac{n(n+1)\alpha}{2} + n\alpha, & (n-1)\alpha + 1 \leqslant x(\tau), \\ \dfrac{(x-1)^2}{2\alpha} + \dfrac{(x-1)}{2}, & 1 \leqslant x(\tau) < (n-1)\alpha + 1, \\ 0, & -1 < x(\tau) < 1, \\ -\dfrac{(|x|-1)^2}{2\alpha} - \dfrac{(|x|-1)}{2}, & -[(n-1)\alpha + 1] < x(\tau) \leqslant -1, \\ -n[|x(\tau)|-1] + \dfrac{n(n+1)\alpha}{2} - n\alpha, & x(\tau) \leqslant -[(n-1)\alpha + 1], \end{cases} \tag{13}$$

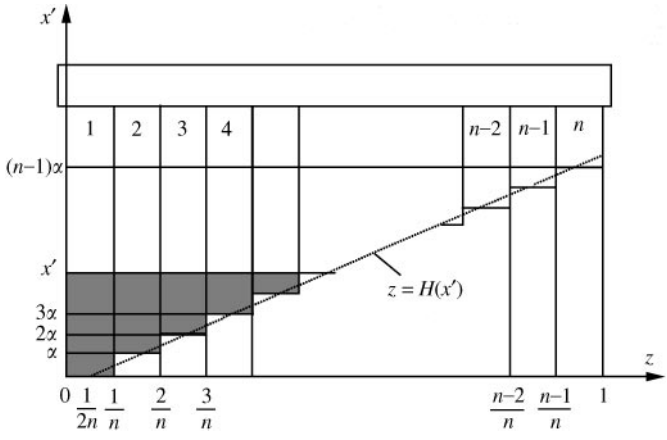

Figure 5. An example of uniformly varying tooth position errors.

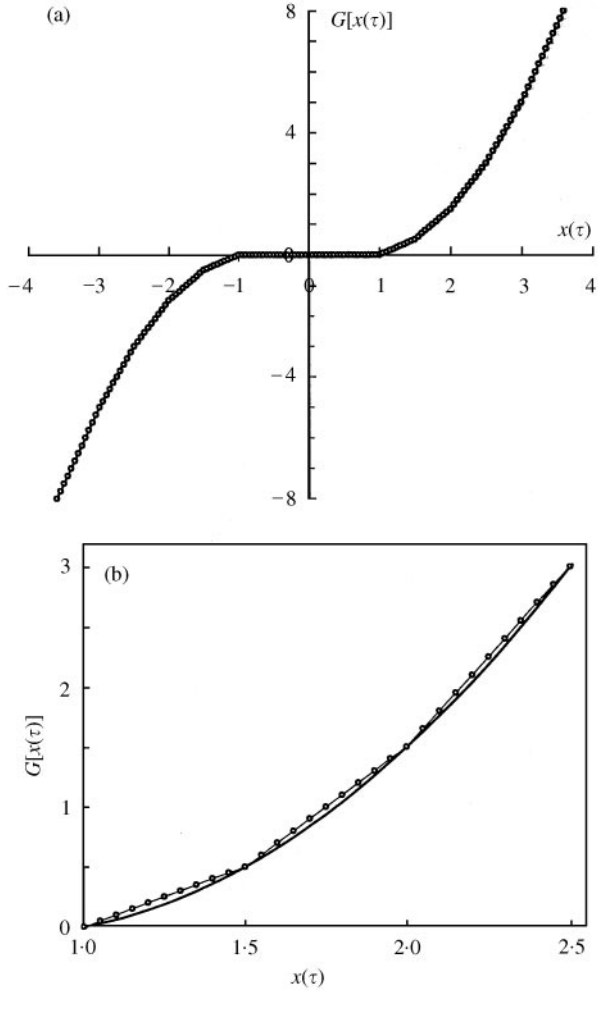

Figure 6. (a) Comparison of exact and approximate forms of $G[x(\tau)]$ for a case of uniformly varying tooth position errors; $n = 5$ and $\alpha = 0{\cdot}5$; (b) zoomed view of a segment in the piecewise linear region: (○), Exact; (——), approximate.

where

$$\sum_{i=1}^{n} \alpha_i = \sum_{i=1}^{n} (i-1)\alpha = \left[\frac{n(n+1)}{2} - n\right]\alpha.$$

In Figure 6(a), the exact and approximate forms of $G[x(\tau)]$ as defined by equations (9) and (13), respectively, are compared for a spline having $n = 5$ with uniformly varying errors of $\alpha = 0{\cdot}5$. Both curves are identical in the region of the backlash ($-1 < x(\tau) < 1$) and in the regions where all teeth are in contact ($|x(\tau)| > 3$), as expected. Within the two regions in between ($1 < |x(\tau)| < 3$), both piecewise linear (exact) and piecewise non-linear (approximation) curves are very close suggesting that the approximate form defined by equation (10) is valid. The slight difference is illustrated in Figure 6(b) that is obtained by blowing up a portion of Figure 6(a) where the differences are the most obvious. It is also evident from Figure 6 that the accuracy of the approximate curve should improve further for splines with larger n.

It is obvious that modelling a spline in a form as given above introduces a type of non-linear system that has not been studied in detail in the past. While continuously non-linear and simple piecewise linear or bi-linear systems have been studied extensively, piecewise non-linear systems like the one defined above by equation (13) for a spline joint have attracted very limited interest [10, 11]. The current research of this author includes deriving analytical solutions to the formulation presented here and also incorporating it in the dynamic analysis of multi-degree-of-freedom drive train systems.

4. CONCLUSION

In this study, a piecewise linear dynamic model of a spline joint subjected to both backlash and circumferential tooth position errors is proposed. The equation of motion with a piecewise linear displacement function is obtained in the dimensionless form. For cases with a large number of spline teeth, a generalized approximation that reduces the piecewise linear displacement function into a piecewise non-linear one is proposed, and its accuracy is demonstrated using a case of linearly varying tooth position errors.

REFERENCES

1. J. E. SHIGLEY 1977 *Mechanical Engineering Design*. Tokyo: McGraw-Hill Kogakusha, Ltd.
2. H. N. OZGUVEN and D. R. HOUSER 1988 *Journal of Sound and Vibration* **121**, 383–411. Mathematical models used in gear dynamics.
3. A. KAHRAMAN and R. SINGH 1991 *Journal of Sound and Vibration* **144**, 469–506. Non-linear dynamics of a geared rotor-bearing system with multiple clearances.
4. A. RAGHOTHAMA and S. NARAYANAN 1999 *Journal of Sound and Vibration* **226**, 469–492. Bifurcation and chaos in geared rotor bearing systems by incremental harmonic balance method.
5. R. SINGH, H. XIE and R. J. COMPARIN 1989 *Journal of Sound and Vibration* **130**. Analysis of automotive neutral rattle.
6. G. W. BLANKENSHIP and A. KAHRAMAN 1995 *Journal of Sound and Vibration* **185**, 743–765. Steady state forced response of mechanical oscillator with combined parametric excitation and clearance type non-linearity.
7. B. MEVEL and J. L. GUYADER 1993 *Journal of Sound and Vibration* **162**, 471–487. Route to chaos in ball bearings.
8. S. THEODOSSIADES and S. NATSIAVAS 2000 *Journal of Sound and Vibration* **229**, 287–310. Non-linear dynamics of gear-pair systems with periodic stiffness and backlash.

9. Q. LIN and J. K. ROKNE 1996 *Computer-Aided Design* **28**, 439–449. Smoothing of piecewise linear splines and the application to piecewise linear fat splines.
10. A. KAHRAMAN and R. SINGH 1992 *Journal of Sound and Vibration* **153**, 180–185. Dynamics of an oscillator with both clearance and continuous non-linearities.
11. Y. WANG 1995 *Journal of Sound and Vibration* **185**, 155–170. Dynamics of unsymmetric piecewise-linear/non-linear systems using finite elements in time.